



PREDICTION OF SCATTERED SOUND FIELD BASED ON THE REVERSAL OF ACOUSTIC DIFFRACTION TOMOGRAPHY

Shuozhong Wang

School of Communication & Information Engineering, Shanghai University, 149 Yanchang Road, Shanghai 200072, China

e-mail: shuowang@shu.edu.cn

In a reversed direction of computer tomography, the Fourier diffraction theorem is used to treat a forward problem in underwater acoustics, that is, prediction of far-field sound scattering from a known object insonified by a plane wave. The cross-sectional distribution of acoustic properties of the scattering target and the surrounding medium is viewed as an image, which is transformed into the frequency domain using 2D FFT. A pair of half-circular arcs in the frequency domain can be specified from the frequency and propagation direction of the incident sound wave. Spectral coefficients of the target image taken from these half-circles are used to calculate the field projections via 1D FFT. Aimed at solving the scattering problem in monostatic settings, this work is focused on the prediction of backscattered sound field. The method is very efficient in computation since, unlike other numerical approaches such as the finite element method (FEM) and the finite-difference time-domain method (FDTD), iterations over the entire computation domain is not needed, and the otherwise highly demanding computation is done with a single 2D FFT operation. Numerical results are provided and compared with FDTD, showing promising prospects of the method.

1. Introduction

A forward problem is to predict the response to a stimulus from the known properties of a system. In underwater acoustics, calculation of the sound pressure distribution, target strength, directional pattern, etc., given the properties of a scattering object insonified by a known incident wave, is a typical forward problem. It can be solved by various means including analytical, asymptotic, and numerical approaches. Since rigorous analytical solutions are rarely possible for practical problems, numerical methods are popular due to their wide applicability and great flexibility. Instead of the frequently used finite element method/boundary element method (FEM/BEM)¹ and the finite-difference time-domain method (FDTD)^{2,3}, we propose a novel technique to predict scattering

from a target based on the application of the Fourier diffraction theorem in a different perspective from its conventional use in solving inverse problems, typically, diffraction tomography.

Diffraction tomography is a variation of computer tomography (CT) for medical diagnoses⁴. CT reconstructs the cross-sectional image of an object from a set of projections generated by X-ray scans. The inventor of the first X-ray CT scanner, Godfrey Hounsfield, and Allan Cormack who independently laid the theoretical foundation of the technique early in the 1960s, jointly received the Nobel Prize in 1979 for their contribution that has profound significance in clinical medicine.

In computer tomography, projection data are related to the 2D Fourier transform of the cross-sectional distribution of the object through the Fourier slice theorem. When acoustic or electromagnetic waves are used, the Fourier diffraction theorem must be used instead since, unlike X-rays, the wavelengths are comparable to the object dimension so that diffraction must be taken into account, hence the term *diffraction CT*⁵. Both forward and backward projections can be used in the reconstruction, referred to as transmission mode diffraction tomography (TMDT) and reflection mode diffraction tomography (RMDT), respectively^{6,7}.

By using the Fourier diffraction theorem in a reversed fashion in contrast to diffraction CT, the method we propose in this paper offers a major advantage in computational efficiency over FEM/BEM and FDTD that involve tremendous iterations on a 2D or 3D grid, and are difficult, if not impossible, to be used in high frequency and/or large object applications. We will briefly introduce the Fourier diffraction theorem, show how it can be used to efficiently calculate the scattered sound given parameters of the incident wave and the scattering object, and make comparison with the FDTD results.

2. Fourier Diffraction Theorem

The diffraction CT is to reconstruct the cross-sectional distribution of an object from information carried by the scattered field that satisfies the Helmholtz equation⁸:

$$(\nabla^2 + k_0^2)u_s(\mathbf{r}) = -k_0^2 o(\mathbf{r})[u_i(\mathbf{r}) + u_s(\mathbf{r})] \quad (1)$$

where $u_i(\mathbf{r})$ and $u_s(\mathbf{r})$ are pressures of the incident and scattered fields, k_0 is the wave number, and $o(\mathbf{r})$ a function representing the object's geometry and acoustic properties. Eq. (1) has the following solution:

$$u_s(\mathbf{r}) = \int g(\mathbf{r} - \mathbf{r}') o(\mathbf{r}') u_i(\mathbf{r}') d\mathbf{r}', \quad u_s \ll u_i \quad (2)$$

where $g(\mathbf{r} - \mathbf{r}')$ is the Green's function. Born or Rytov approximation is used based on an assumption of weak scattering^{4,9}. The Fourier diffraction theorem can be derived by taking Fourier transform of both sides of Eq. (2).

Assuming the incident plane wave is propagated towards the positive x -axis, the one dimensional Fourier transform of the forward/backward projection taken on a line parallel to the y -axis and crossing the x -axis at $x = l_0$ is

$$U_s^{(\alpha=l_0)}(k_y) = \frac{j}{2\sqrt{k_0^2 - k_y^2}} O\left(\alpha\sqrt{k_0^2 - k_y^2} - k_0, k_y\right) \exp\left(j l_0 \sqrt{k_0^2 - k_y^2}\right), \quad |k_y| < k_0 = \sqrt{k_x^2 + k_y^2} \quad (3)$$

where $\alpha = 1$ and $\alpha = -1$ correspond to forward and backward projections respectively. One can see from Eq. (3) that, for the forward projection, U_s is a sequence of samples located on a half-circle in the 2D Fourier domain with a radius k_0 , centered at $k_x = -k_0$ and $k_y = 0$, and tangent to the vertical axis at the origin. For the backward projection, the samples are located on the complement of the above half-circle, which passes through the horizontal axis at $k_x = -2k_0$.

The theorem can be explained in a diagrammatic manner as illustrated in Fig. 1. A vector of forward projection, \mathbf{p}_F , is obtained by measuring the scattered sound along the line T_1T_1' when the

object is insonified by a plane wave of angular frequency ω_0 , propagating in the direction measured by an angle φ . The one dimensional DFT of \mathbf{p}_F gives samples on a half-circle in the object's two dimensional DFT, depicted as the thick curve (low frequency half-circle) in the right part of Fig. 1. This is TMDT. Radius of the half-circle equals the spatial frequency of the incident wave, $k_0 = \omega_0/c$, in radians per meter. When k_0 approaches infinity, the radius tends to infinity so that the half-circle becomes a straight line, and the theorem degenerates to the Fourier slice theorem for the X-ray CT. In the case of RMDT, the backward projection \mathbf{p}_B taken along T_2T_2' corresponds to the samples on the high frequency half-circle depicted as the thick dotted curve in Fig. 1. If ordinary frequency is used instead of angular frequency as in the numerical computation described in the following, the spatial frequency axes in Fig. 1 should be changed to $1/\lambda_x$ and $1/\lambda_y$ and the radius of the half-circles becomes $1/\lambda_0$.

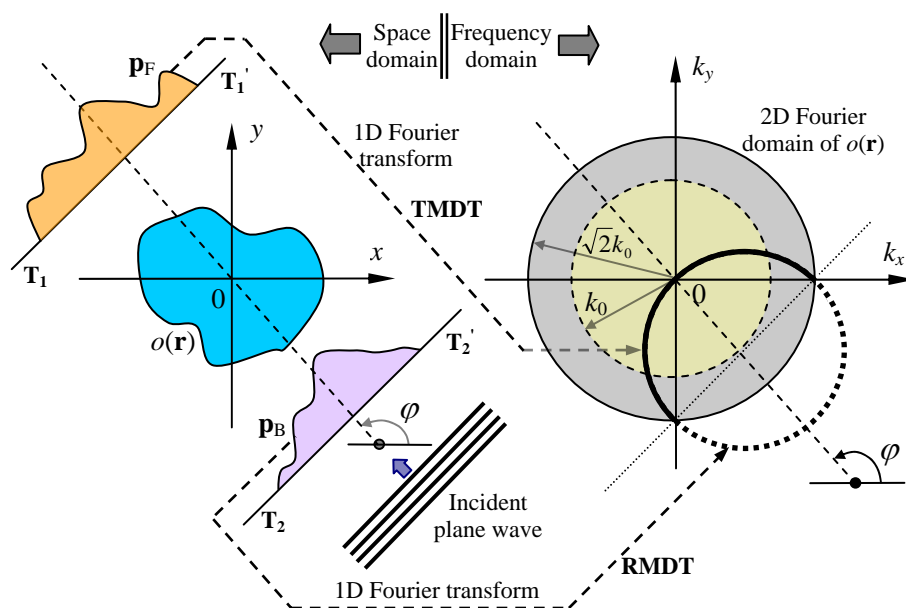


Figure 1. Schematic diagram explaining the Fourier diffraction theorem

3. Prediction of Scattered Sound

Our purpose is to apply the Fourier diffraction theorem in a reversed fashion with respect to the diffraction CT, in other words, to calculate scattered sound from the geometric and acoustic parameters of an object insonified by a plane wave. We will mainly focused on backscattering in the present work. To confine the discussion to a 2D problem, assume that a cylindrical object is immersed in water with the incident direction perpendicular to its axis. Consider a cross-section of the cylinder and the surrounding water:

$$o(\mathbf{r}) = \rho(\mathbf{r})c(\mathbf{r}) \quad (4)$$

where $\rho(\mathbf{r})$ is the density and $c(\mathbf{r})$ the sound velocity, both functions of the spatial coordinates \mathbf{r} . Consider a rectangular region that encloses the object and the surrounding water. Discretize the function $o(\mathbf{r})$ in the rectangular region by sampling it on a square grid, with an inter-sample spacing $\delta = \lambda_0/L$ where λ_0 is the wavelength and L a positive integer, and then quantize the ρc values to B bits. Thus we obtain a digital image \mathbf{o} , and its DFT, \mathbf{O} , containing information of the object. Fig. 2(a) shows the discretized cross-section of an elliptical cylinder made of steel and surrounded by sea water, and Fig. 2(b) the magnitude of its DFT in a form of digital image, scaled and quantized to fit the range of display, usually $[0, 255]$. We know that the Fourier transform of an ellipse is also elliptic in shape. Irregularity in the high frequency region is a result of the zigzagging edge of

the sampled object due to finite discretization steps. Sampling and quantization will introduce some numerical errors as will be observed below.

We let the incident plane wave propagate along the positive x axis, thus $\varphi = 0$. According to the Fourier diffraction theorem, the frequency domain samples on the solid and dotted half-circles in Fig. 2(b) correspond to the forward and backward projection, respectively, in the space domain. Parameters of the incident wave, the scattering object and the surrounding medium, and the size of the rectangle and the sampling grid are listed in Table 1. In the table, four elliptical cylinders with different sizes are listed that are used in the computation, in which (a)-(c) are made of steel and (d) made of aluminium.

Since $\lambda_0 = 1$ m and $L = 8$, the sampling interval in the space domain is $\delta = \lambda_0/L = 0.125$ m. For the square area sized $15\text{m} \times 15\text{m}$ in Fig. 2, the total number of samples is $N^2 = 121 \times 121$, the frequency domain sampling interval is $\delta f = 1/15 \text{ m}^{-1}$, and therefore the frequency range as plotted in Fig. 2(b) is $W \times W$ where $W = (N-1)\delta f = 8 \text{ m}^{-1}$. With the DC component shifted to the center, ranges of spatial frequencies both in the horizontal and vertical directions in Fig. 2(b) are $[-4, 4] \text{ m}^{-1}$. The radius of the half-circles is $1/\lambda_0 = 1 \text{ m}^{-1}$. Samples taken from the solid and dotted half-circles corresponding to the forward and backward projections, respectively, are plotted in Fig. 3.

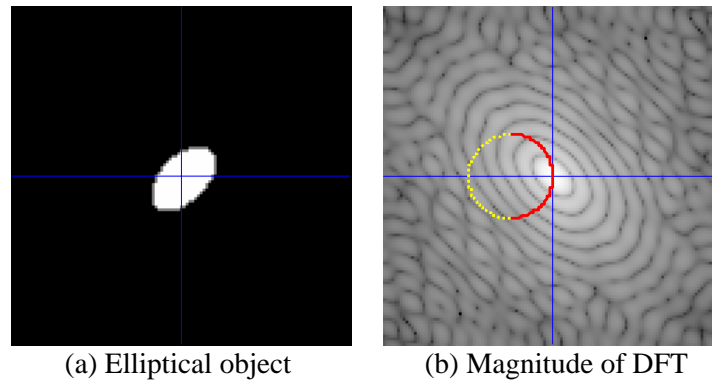


Figure 2. Cross-sectional image of a steel cylinder and its 2D Fourier transform. Size of the square area is $15 \times 15 \text{ m}^2$, and the frequency range is $[-4, 4] \text{ m}^{-1}$. The solid and dotted half-circles show locations where the Fourier domain samples are taken for calculating the forward and backward projections in the space.

Table 1. Physical, geometrical, and numerical parameters used in computation with four elliptical cylinders among which (a)-(c) are made of steel and (d) made of aluminium corresponding to the plots in Fig. 4

| Name | Symbol | Unit | Values | | | |
|------------------------------------|------------------------|----------------------|--------|-----------------------|-----|----------------------|
| | | | (a) | (b) | (c) | (d) |
| Long axis | a | m | 1.7 | 2.8 | 2.8 | 1.7 |
| Short axis | b | m | 0.9 | 1.0 | 1.7 | 0.3 |
| Density of object | ρ_o | kg/m^3 | | 7800 | | 2700 |
| Sound speed in object | c_o | m/s | | 5653 | | 3672 |
| Young's modulus | E | Newton/ m^2 | | 19.5×10^{10} | | 7.1×10^{10} |
| Poisson's ratio | ν | – | | 0.28 | | 0.33 |
| Frequency of incident wave | f_0 | Hz | | 1500 | | |
| Density of water | ρ | kg/m^3 | | 1026 | | |
| Sound speed in water | c | m/s | | 1500 | | |
| Wavelength | $\lambda_0 = c/f_0$ | m | | 1.0 | | |
| Sample number per wavelength | n | – | | 8 | | |
| Interval of spatial sampling | $\delta = \lambda_0/n$ | m | | 1/8 | | |
| Size of square under consideration | $A_x \times A_y$ | m^2 | | 15×15 | | |
| Sample number in a projection | $N = [A_x/\delta] + 1$ | – | | 121 | | |
| Interval of frequency sampling | $\delta f = 1/A_x$ | m^{-1} | | 1/15 | | |

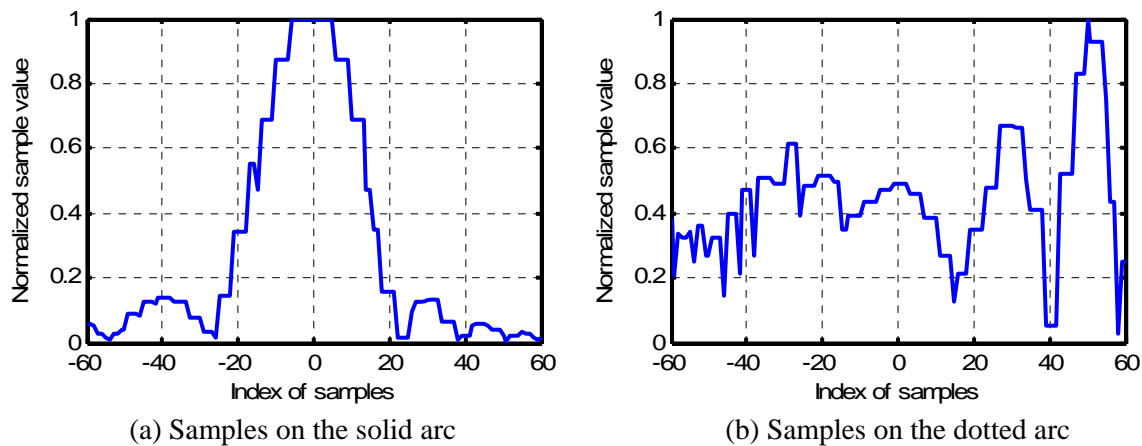


Figure 3. Two sets of spectral samples taken from the half-circular arcs as shown in Fig. 2(b), normalized over each set of the data.

We now rotate the cylinder about its central axis from 0° to 360° and, and perform 2D Fourier transform of the cross-sectional image at every 2° . Each time, we take the Fourier domain samples from the half-circle corresponding to the reflection mode diffraction tomography, and calculate the backward projection by inverse Fourier transform of the sample sequence. From the projection, we obtain the back-scattered sound pressure by averaging the central section of the projection. The number of samples in the section used for averaging is 10% of the total to give a trade-off between accuracy and smoothness.

The results are shown by the solid curves in Figs. 4(a)-4(d), with parameters of the scattering objects and the incident sound wave given in Table 1. The results are compared with those obtained by using FDTD, shown as the dash-dotted curves in the plots. In the FDTD computation, we chose a computation domain that is a square region around the scattering object sized $A^2 = 8 \times 8\text{m}^2$, and a grid size $d = \lambda_0/15 = 0.0667\text{m}$. Note that the grid spacing must be sufficiently small, generally one tenth of the wavelength or less, to ensure an adequate sampling. Thus the total number of grid cells in each side of the square was $N = \text{round}(A/d) + 1 = 121$. To obtain the dash-dotted curve in each of these plots, the sound pressure distribution within the computation domain was calculated for all the orientations of the target, in steps of 1° . In each step, as many as 600 iterations were executed to achieve a stable field. The far field back-scattered pressure was then obtained by near-field/far-field transformation. A unified FDTD algorithm¹⁰ and a least square absorbing boundary condition¹¹ were used in the computation.

It can be observed from Fig. 4 that the results obtained using the proposed Fourier diffraction theorem approach and those of FDTD are generally in a satisfactory agreement. Discrepancy and fluctuations were partly caused by the ruggedness of the coarse sampling of the object and the sound field.

The most important advantage of the proposed method is in the computation efficiency. In the FDTD computation carried out for comparison, a total of $600 \times 360 = 21,600$ iterative operations were performed to get the near-field distributions needed for calculating the scattered sound in the far-field for every step of the iteration. In each step, sound pressure and particle velocity on a 121×121 grid were calculated. With an Intel Centrino processor and 2GB memory running Matlab, 8,000~10,000 seconds were consumed to generate each of the dash-dotted curves in Fig. 4. At high frequencies and with a large scattering target, the computation load would be increasing steeply. In contrast, by using the Fourier diffraction theorem approach proposed in this work, the projections can be obtained without calculating the entire near-field distribution, and the highly efficient fast Fourier transform is performed rather than computationally expensive iterations. To obtain one curve in Fig. 4, about 22 seconds were used, achieving a time saving of more than two orders of magnitude.

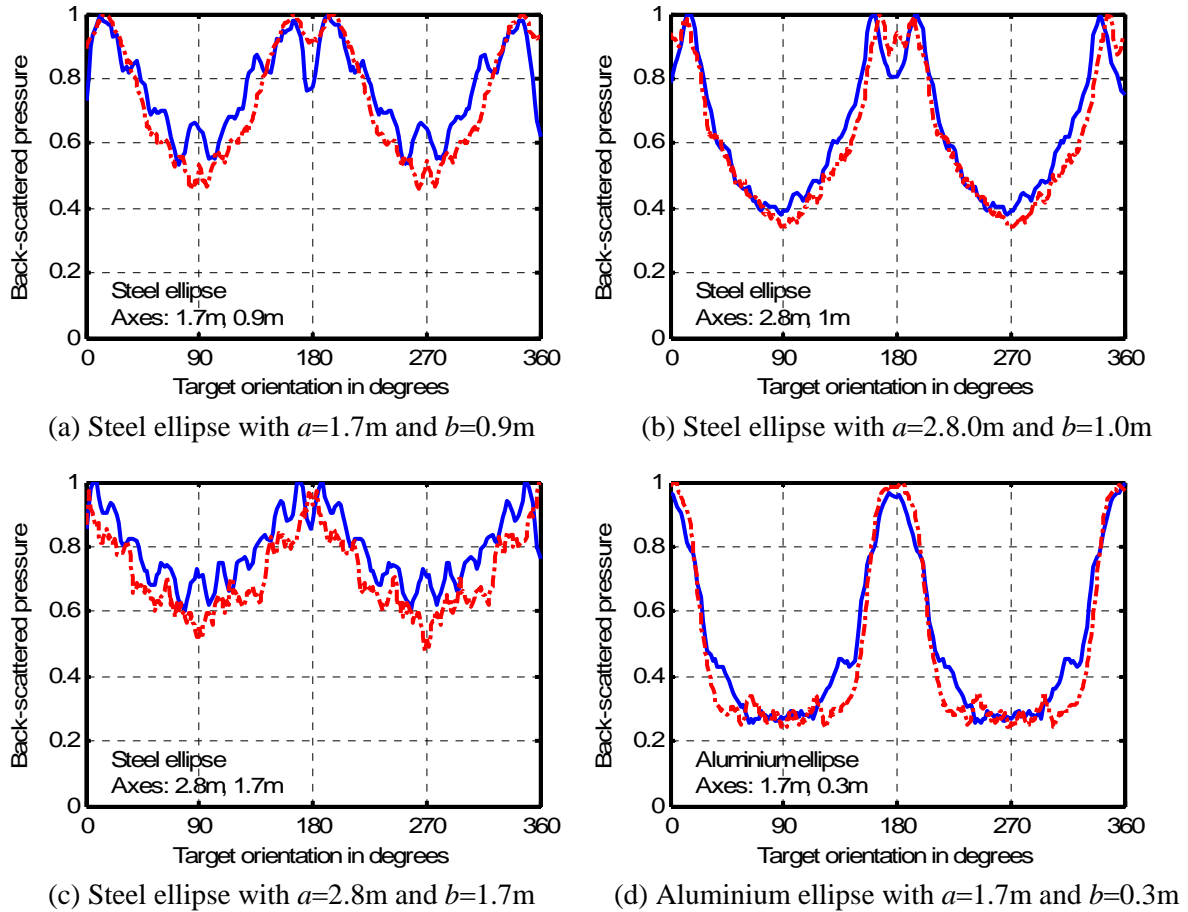


Figure 4. Normalized sound pressure back-scattered by elliptical cylinders made of steel or aluminium, rotating from 0° to 360° , obtained using the proposed Fourier diffraction theorem method (solid) and FDTD (dash-dotted) respectively. Parameters of the objects and the incident wave are listed in Table 1.

4. Conclusions

We propose to use the Fourier diffraction theorem in a reversed manner with respect to the diffraction tomography to solve a forward problem in acoustics: prediction of the scattered sound field from a known incident plane wave and the geometry and physical properties of the scattering object. The reversed application of the Fourier diffraction theorem offers a significant advantage in computation efficiency compared to the popular lattice-based numerical methods, typically FEM/BEM and FDTD. The substantial reduction in the computation burden is achieved by avoiding redundant computation of the entire distribution in the near-field, and using fast Fourier transform in stead of time-consuming iterative operations. Therefore the method is highly efficient and suitable for practical applications.

The scattered sound field is a solution of the wave equation. In essence, FDTD solves the wave equation by imitating the process of wave propagation in an iterative manner, while the method proposed in this work partially solves the wave equation by exploring interaction between the sound wave and the scattering object. It is understood that all information of the object and its surrounding medium is contained in the two-dimensional Fourier transform of the cross-sectional image, and all information of the incident wave, namely, the frequency and the incident angle, is in the radius and location of the half-circle for sampling in the spatial transform domain. Taking spectral samples from a particular half-circle and performing one-dimensional inverse Fourier transform of these samples reveals interaction between the incident sound wave and the scattering object, and therefore is equivalent, in part, to solving the wave equation in obtaining the desired solution to the scattering problem.

Further studies are in order, some of the problems being considered including improvement of the numerical accuracy, more complicated, yet practical situations such as non-sinusoidal and non-plane wave incidence, three-dimensional situations, and bi-static settings.

REFERENCES

- [1] M. Zampolli, F. B. Jensen, and A. Tesei, "Benchmark problems for acoustic scattering from elastic objects in the free field and near the seafloor", *Journal of the Acoustical Society of America* **125**(1), 89-98 (2009)
- [2] S. Wang, "Finite-difference time-domain approach to underwater acoustic scattering problems", *Journal of the Acoustical Society of America* **99**(4), pt.1, 1924-1931 (1996)
- [3] M. M. Shabat, N. M. Barakat, S. Al-Azab and D. Jager, "Finite difference time domain analysis of two dimensional planer scatter", *Proceedings of SPIE* **4829**, 251-252 (2003)
- [4] A. C. Kak, "Computed tomography with X-ray, emission, and ultrasound sources", *Proceedings of the IEEE* **67**, 1245-1272 (1979)
- [5] M. M. Bronstein, A. Bronstein and M. Zibulevsky, "Reconstruction in diffraction ultrasound tomography using non-uniform FFT," *IEEE Transactions on Medical Imaging* **21**, 1395-1401 (2002)
- [6] X. Pan and M. A. Anastasio, "On a limited-view reconstruction problem in diffraction tomography," *IEEE Transactions on Medical Imaging* **21**, 413-416 (2002)
- [7] Z. Y. Tao, Z. Q. Lu, and X. Wang, "Acoustical diffraction tomography in a finite form based on the Rytov transform", *IEEE Transactions on Image Processing* **15**(6), 1264-1269 (2006)
- [8] A. C. Kak and M. Slaney, *Principles of computerized tomographic imaging*, 203-273, IEEE Press, New York, 1999
- [9] S. X. Pan and A. C. Kak, "A computational study of reconstruction algorithm for diffraction tomography: interpolation versus filtered back propagation", *IEEE Transactions on Acoustics, Speech and Signal Processing* **31**, 1262-1275 (1983)
- [10] S. Wang, R. Wang and Z. Fang, "Calculation of sound scattering from elastic targets using unified FDTD formulae", *The 136th Meeting of the Acoustical Society of America*, Norfolk, Virginia, USA, 12-16 October 1998, in *Journal of the Acoustical Society of America* **104**(3), pt.2, 1755 (1998)
<http://www.ci.shu.edu.cn/shuowang/papers/13%20Calculation%20of%20Sound.pdf>
- [11] S. Wang, "An efficient absorbing boundary for finite-difference time-domain field modeling in acoustics", *Chinese Journal of Acoustics* **16**(2), 121-134 (1997)